MECHANICS OF COHESIVE-FRICTIONAL MATERIALS
Mech. Cohes.-Frict. Mater. 2000; **5**:325–339

Fracture evolution during indentation of a brittle elastic solid

A. P. S. Selvadurai*

Department of Civil Engineering and Applied Mechanics, McGill University, 817 Sherbrooke Street West, Montreal, QC, Canada H3A 2K6

SUMMARY

This paper examines the problem of crack extension during the indentation of a brittle elastic half-space by a cylindrical punch with a smooth flat contact surface. The paper develops a procedure for locating the point of nucleation of the crack within the brittle elastic solid and employs a boundary element technique to locate the progress of crack evolution as the force on the punch is increased. The numerical results illustrate the influence of the extent of crack development on the load–displacement relationship for the indentor. Copyright © 2000 John Wiley & Sons, Ltd.

1. INTRODUCTION

The classical problem related to the indentation of the surface of an isotropic elastic half-space region by a smooth rigid flat indentor with a circular plan form was first examined by Boussinesq[1] using the mathematical similarity between results of potential theory and the analogous formulation of boundary value problems in classical elasticity theory. The problem was re-examined in a celebrated paper by Harding and Sneddon,[2] who reduced the mixed boundary value problem to a system of dual integral equations and their further reduction to an integral equation of the Abel-type. Harding and Sneddon[2] also obtained the load–displacement relationship for the rigid indentor in exact closed form. A number of distinguished mathematicians and engineers including Hertz[3] and Love[4] have also developed solutions to the problem of the indentation of half-space regions with anisotropic and non-homogeneous elastic properties by indentors having arbitrary surface profiles. The body of literature on classical elastostatic problems on contact mechanics is quite extensive and references to important developments covering mathematical, computational and experimental aspects are given by Galin,[5] Ufliand,[6] de Pater and Kalker,[7] Selvadurai,[8] Gladwell,[9] Johnson[10] and Kalker.[11]

In all classical studies involving indentation problems, it is implicitly assumed that the originally intact half-space region will remain intact during the indentation process. Such an assumption is likely to be valid for situations involving indentation of relatively flexible materials which can maintain their elastic continuum character even in regions of high-stress concentrations. With the classical linear elasticity formulation, the stress field at regions where there is a discontinuity in the displacement field imposed by the indentation will exhibit singular behaviour. When the mechanical behaviour of the indented material is predominantly brittle elastic, regions of such high-stress concentrations are prone to brittle fracture.[12–15] The

* Correspondence to: A. P. S. Selvadurai, Department of Civil Engineering and Applied Mechanics, McGill University, 817 Sherbrooke Street West, Montreal, QC, Canada H3A 2K6.

Received 20 December 1998
Revised 17 May 1999

occurrance of such brittle fracture phenomena during Hertzian indentation of brittle elastic solids has been observed by a number of investigators including Tillett,[16] Roesler,[17,18] Frank and Lawn,[19] Lawn[15] and Chen *et al.*[20] The theory of the Hertzian indentational fracture problem was investigated by Frank and Lawn,[19] Chaudhri and Yoffe,[21] and Keer *et al.*[22] using analytical procedures. Yingzhi and Hills (1991) and Chen *et al.*[20] have used finite element techniques to examine the indentational fracture problem. In these studies, the role of surface flaws in initiating the fracture is examined in detail. In a critical review of the indentational fracture problem Lawn and Wilshaw,[23] Ostojic and McPherson[24] note that the types of fractures can be varied and to a large extent influenced by surface defects that can either be present or introduced during the preparation of the surface. It is also foreseeable that shrinkage effects and other thermo-mechanical processes can also influence the development of surface defects which will in turn influence both the type and growth of cracks during the indentation process. The fracture types can include either semi-circular two-dimensional flat cracks, or cracks with a star-shaped plan form or curved cracks with a conoidal surface.

In this paper we investigate the problem of fracture initiation and extension at the boundary of a Boussinesq-type smooth flat indentor with a circular plan form. The analysis utilizes the results for the stress state at the boundary of the rigid indentor to identify the location and orientation of the crack initiation. The starter crack is allowed to extend in an axisymmetric conoidal form (Figure 1) through specified crack extension and orientation of crack extension criteria. The analysis utilizes a boundary element technique to capture the quasistatic growth of the crack with

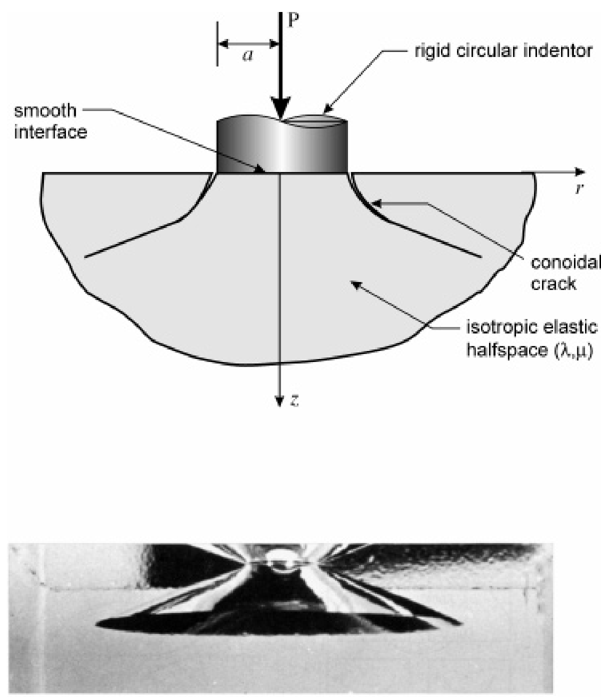

[After Roesler, 1956a]

Figure 1. Surface fracture generation during indentation

an increase in the resultant axial load applied to the rigid circular indentor. The results of the analysis indicates that the pattern of axisymmetric conoidal crack growth is influenced by Poisson's ratio of the brittle elastic solid and that the load–displacement behaviour of the indentor can exhibit a non-linear response which can be attributed to the progressive extension of the conoidal crack.

2. COMPUTATIONAL MODELLING OF FRACTURE DEVELOPMENT

We consider the axisymmetric indentation of the surface of an isotropic elastic half-space region by a smooth flat rigid indentor of radius a. The objective of the computational modelling is to develop a methodology which can predict the process of quasi-static crack extension from the boundary of the indentor. The analysis of crack extension during indentation can be performed via a variety of computational schemes. These can include either finite element methods or boundary integral equation methods or their combinations. The application of finite element techniques to fracture extension is well established; it requires the specification of criteria both for the initiation of crack extension and for the orientation of crack extension. These relationships which are applicable to brittle elastic fracture initiation and extension are readily available in the literature in fracture mechanics.[25,26] In the modelling of crack extension via the finite element method, remeshing is an important feature that ensures accuracy of both local and global stress fields. In recent years adaptive remeshing techniques have been used quite effectively to examine crack extension in brittle geomaterials such as concrete and rock.[13,27,28] An alternative to remeshing involves extensive irregular mesh refinement in the vicinity of the singular crack tip element and allows crack extension to take place at element boundaries.[29] There are however alternative schemes, such as the boundary element method which provides greater flexibility when examining the process of crack extension. The primary advantage of integral equation-based concepts such as the boundary element method or the displacement discontinuity method, is that the domain rearrangement resulting from the crack extension process requires only a nominal incremental change in the boundary element mesh or the displacement discontinuity line along the crack extension path. For this reason, we shall adopt here the boundary element scheme to examine the process of quasi-static conoidal crack extension during the indentation process. The application of boundary element schemes to problems in fracture mechanics originated with the work of Cruse and Wilson[30] and extended by a number of other investigators including Blandford *et al.*,[31] Smith and Mason,[32] Selvadurai and Au,[33] Selvadurai[34–36] and Selvadurai and ten Busschen[37] to include a variety of problems including cracks with frictional interfaces. A recent review article by Aliabadi[38] gives a comprehensive survey of research related to boundary element formulations in fracture mechanics conducted over the past two decades.

We consider the axisymmetric indentational fracture of a brittle elastic isotropic half-space region which satisfies Hooke's Law

$$\sigma_{ij} = \lambda \delta_{ij} u_{k,k} + \mu \{u_{i,j} + u_{j,i}\} \tag{1}$$

and the Navier equations

$$\mu \nabla^2 u_i + (\lambda + \mu) u_{k,ki} = 0 \tag{2}$$

where μ and λ are Lamé's constants, u_i and σ_{ij} are, respectively, the displacement components and the stress tensor referred to the rectangular Cartesian co-ordinate system x, y, z; $\lambda(= 2\mu/(1 - 2v))$

and $\mu(=E/2(1+\nu))$ where E is Young's modulus and ν is Poisson's ratio; δ_{ij} is Kronecker's delta function and ∇^2 is Laplace's operator. The boundary integral equation governing axisymmetric deformations can be written as

$$c_{\ell k} u_k + \int_\Gamma \{P^*_{\ell k} u_k + u^*_{\ell k} P_k\} \frac{r}{r_i} \, \mathrm{d}\Gamma = 0 \tag{3}$$

where Γ is the boundary of the domain; u_k and P_k are, respectively, displacements and tractions on Γ and u^*_{ik} and P^*_{ik} are fundamental solutions.[30,39] In (3), $c_{\ell k}$ is a constant which can take values of either zero (inside the domain); $\delta_{ij}/2$ (if the point is located at a smooth boundary) or a function of the discontinuity at a corner and of Poisson's ratio. For axial symmetry, the displacement fundamental solutions can take the form

$$u^*_{rr} = C_1 \left\{ \frac{4(1-\nu)(\rho^2+\bar{z}^2)-\rho^2}{2r\bar{R}} \right\} K(\bar{m}) - \left\{ \frac{(7-8\nu)\bar{R}}{4r} - \frac{(e^4-\bar{z}^4)}{4r\bar{R}^3 m_1} \right\} E(\bar{m}) \tag{4}$$

$$u^*_{rz} = C_1 \bar{z} \left\{ \frac{(e^2+\bar{z}^2)}{2\bar{R}^3 m_1} E(\bar{m}) - \frac{1}{2\bar{R}} K(\bar{m}) \right\} \tag{5}$$

etc., where

$$\bar{z} = (z - z_i), \quad \bar{r} = (r + r_i), \quad \rho^2 = (r^2 + r_i^2)$$
$$e^2 = (r^2 - r_i^2), \quad \bar{R}^2 = \bar{r}^2 + \bar{z}^2, \quad C_1 = \frac{1}{4\pi\mu(1-\nu)} \tag{6}$$
$$\bar{m} = \frac{4rr_i}{\bar{R}^2}, \quad m_1 = 1 - \bar{m}$$

$K(\bar{m})$ and $E(\bar{m})$ are, respectively, complete elliptic integrals of the first and second kind and (r, z) and (r_i, z_i) correspond to the coordinates of the *field* and *source* points, respectively. The appropriate expressions for the traction fundamental solution $P^*_{\ell k}$ can be obtained by the manipulation of the results of type (4) and (5). If we consider a discretization of the boundary Γ, the integral equation (3) can be expressed in the form of a boundary element matrix equation as follows:

$$[\mathbf{D}]\{\mathbf{U}\} = [\mathbf{T}]\{\mathbf{P}\} \tag{7}$$

where $[\mathbf{D}]$ and $[\mathbf{T}]$ are derived from the integration of the displacement and traction fundamental solutions, respectively.

When considering the discretization of the boundary Γ of the domain, quadratic elements can be employed quite successfully. The variations of the displacements and tractions within an element can be described by

$$\left. \begin{matrix} u_i \\ P_i \end{matrix} \right\} = a_0 + a_1\zeta + a_2\zeta^2 \tag{8}$$

where ζ is the local co-ordinate of the element and a_r $(r = 0, 1, 2)$ are arbitrary constants of interpolation. When modelling cracks which occur at the boundaries or within the interior of the elastic medium, it is necessary to modify (8) to take into consideration the $1/\sqrt{\zeta}$-type stress

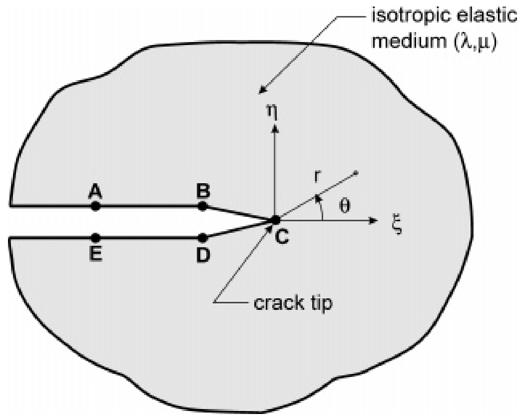

Figure 2. Crack tip geometry and node locations

singularity at the crack tip. In the finite element method, quarter-point elements of the type proposed by Henshell and Shaw[40] and Barsoum[41] can be used to model the required $\sqrt{\zeta}$-type variation in the displacement. If the same type of element is implemented in a boundary element scheme, i.e.

$$\left.\begin{matrix} u_i \\ P_i \end{matrix}\right\} = b_0 + b_1\sqrt{\zeta} + b_2\zeta \tag{9}$$

where b_i $(i = 0, 1, 2)$ are constants, the required stress singularity cannot be duplicated. Cruse and Wilson[30] introduced the so-called '*singular traction quarter-point boundary element*', where the tractions in (9) are multiplied by a non-dimensional $\sqrt{\ell_0/\zeta}$, where ℓ_0 is the length of the crack-tip element. The variations in the tractions can thus be expressed in the form

$$P_i = \frac{c_0}{\sqrt{r}} + c_1 + c_1\sqrt{r} \tag{10}$$

where c_i $(i = 0, 1, 2)$ are constants. Singular traction quarter-point boundary elements have been extensively applied to the boundary element modelling of crack problems and their accurate performance is well documented.[33,36,38] In the context of the present paper, an objective of the computational modelling is to determine both Modes I and II stress intensity factors which are necessary to accurately establish the processes of both initiation of crack extension and orientation of crack extension. For axial symmetry only Modes I and II stress intensity factors can be present and these can be determined by applying a displacement correlation method which makes use of the nodal displacements at four locations *A B*, *E* and *D* and the crack tip (Figure 2), i.e.

$$K_{\mathrm{I}} = \frac{\mu}{(k+1)}\sqrt{\frac{2\pi}{\ell_o}}\{4[u_\eta(B) - u_\eta(D)] + [u_\eta(E) - u_\eta(A)]\} \tag{11}$$

$$K_{\mathrm{II}} = \frac{\mu}{(k+1)}\sqrt{\frac{2\pi}{\ell_o}}\{4[u_\xi(B) - u_\xi(D)] + [u_\xi(E) - u_\xi(A)]\} \tag{12}$$

where $k = (3 - 4\nu)$ and ℓ_0 is the length of the crack tip element. In the current numerical simulations, quarter-point elements are used to model the crack tip fields and substructuring techniques are used to model the region containing the crack.

3. MODELLING OF CRACK EXTENSION

The computational methodology described in the previous section can be applied to examine the mechanics of crack extension during brittle fracture. To apply the computational scheme, it is necessary to establish criteria which describe (i) the nucleation of cracks, (ii) the initiation of crack extension and (iii) the orientation of crack extension.

3.1. Crack nucleation

The continuum idealization of the brittle material precludes the existence of micro-cracks or defects of any size within the 'continuum scale'. Therefore, the process of crack nucleation has to be approached by specifying a stress condition which permits the development of a surface of discontinuity within the material. As observed by Lawn,[15] the accurate determination of crack nucleation requires the consideration of processes at the microstructural level and the associated criteria cannot be formulated with precision. In the context of the indentational fracture problem, the stress state in an intact continuum region will be examined to determine the location of nucleation of a *precursor-crack*. Such elementary crack initiation criteria have been used quite extensively to introduce '*crack nucleation*' in an otherwise defect-free continuum. With regard to the Boussinesq-type indentation problem, in order to identify the location of crack nucleation it is necessary to evaluate the local stress field within the half-space in the vicinity of the boundary of the flat indentor.

We consider the problem of the axisymmetric indentation of the surface of an isotropic elastic half-space by a smooth flat rigid indentor of radius a. The resulting mixed boundary value problem is given by

$$\begin{aligned} u_z(r,z) &= \Delta, \quad 0 \leqslant r \leqslant a, \quad z = 0 \\ \sigma_{zz}(r,z) &= 0, \quad a < r < \infty, \quad z = 0 \\ \sigma_{rz}(r,z) &= 0, \quad 0 \leqslant r < \infty, \quad z = 0 \end{aligned} \tag{13}$$

where u_r and u_z are the displacement components referred to the (r, θ, z) co-ordinate system and σ_{zz}, σ_{rz} are the stress components. The solution to the mixed boundary value problem is given by Harding and Sneddon[2] and Sneddon[42] and the state of stress within the half-space region can be expressed in the following forms:

$$\sigma_{zz}(r,z) = -\frac{4\mu(\lambda+\mu)\Delta}{(\lambda+2\mu)\pi a}\,\{J_1^0 + \xi J_2^0\} \tag{14}$$

$$\sigma_{\theta\theta}(r,z) = -\frac{4\lambda\mu}{(\lambda+2\mu)}\frac{\Delta}{\pi a}\{J_1^0\} - \frac{4\mu^2}{\tilde{\rho}(\lambda+2\mu)}\left\{J_0^1 - \frac{(\lambda+\mu)}{\mu}\,\xi J_1^1\right\} \tag{15}$$

$$\sigma_{rr}(r,z) + \sigma_{\theta\theta}(r,z) = -\frac{4\mu}{(\lambda+2\mu)}\frac{\Delta}{\pi a}\{(2\lambda+\mu)J_1^0 - (\lambda+\mu)\xi J_2^0\} \tag{16}$$

$$\sigma_{rz}(r,z) = -\frac{4\mu(\lambda+\mu)}{(\lambda+2\mu)}\frac{\Delta}{\pi a}\,\xi J_2^1 \tag{17}$$

where

$$J_n^m = \int_0^\infty p^{n-1} \sin(p) e^{-p\xi} J_m(\tilde{\rho} p)\, dp \tag{18}$$

and $J_m(x)$ is the Bessel function of the first kind of order m. The integrals in (18) can be evaluated in an analytical form as follows:

$$\begin{aligned} J_1^0 &= R^{-1/2} \sin\left(\frac{\phi}{2}\right) \\ J_2^0 &= rR^{3/2} \sin\left(\frac{3\phi}{2} - \theta\right) \\ J_0^1 &= \frac{1}{\tilde{\rho}}\left[1 - R^{1/2}\sin\left(\frac{\phi}{2}\right)\right] \\ J_2^1 &= \tilde{\rho} R^{-3/2}\sin\left(\frac{3\phi}{2}\right). \end{aligned} \tag{19}$$

where

$$\begin{aligned} r^2 &= 1 + \xi^2, \quad \tan\theta = \frac{1}{\xi} \\ R^2 &= (\tilde{\rho}^2 + \xi^2 - 1)^2 + 4\xi^2 \\ \tan\phi &= \frac{2\xi}{(\tilde{\rho}^2 + \xi^2 - 1)} \end{aligned} \tag{20}$$

and $\tilde{\rho}$ and ξ are the dimensionless co-ordinates

$$\tilde{\rho} = \frac{r}{a}; \quad \xi = \frac{z}{a} \tag{21}$$

The local stress field beneath the rigid circular indentor (Figure 3) can be obtained from the result

$$\sigma_{\psi\psi} = \sigma_{rr} \sin^2\psi + \sigma_{zz} \cos^2\psi - 2\sigma_{rz} \sin\psi \cos\psi \tag{22}$$

$$\sigma_{\eta\eta} = \sigma_{rr} \cos^2\psi + \sigma_{zz} \sin^2\psi + 2\sigma_{rz} \sin\psi \cos\psi \tag{23}$$

$$\sigma_{\eta\psi} = \frac{(\sigma_{rr} - \sigma_{zz})}{2} \sin 2\psi + \sigma_{rz} \cos 2\psi \tag{24}$$

The maximum local tensile stress within the elastic medium, in the vicinity of the boundary of the indentor can be obtained by a computationally based search technique. The location of the point of maximum tensile stress will be characterized by the local co-ordinates of η_0 and ψ_0 and will be dependent only on Poisson's ratio of the brittle elastic material. Figure 4 illustrates the variation of ψ_0 and η_0/a as a function of $v \in (0, 0{\cdot}5)$. It is evident that the location of maximum tensile stress is well defined except at values of $v \to 1/2$. The type of brittle elastic materials which are prone to brittle fracture generation will generally have $v < 1/2$; as a result, the elastic stress state in the vicinity of the boundary of the rigid circular indentor could be used to determine the location of maximum tensile stress in that region. It is assumed that the crack nucleates at the location

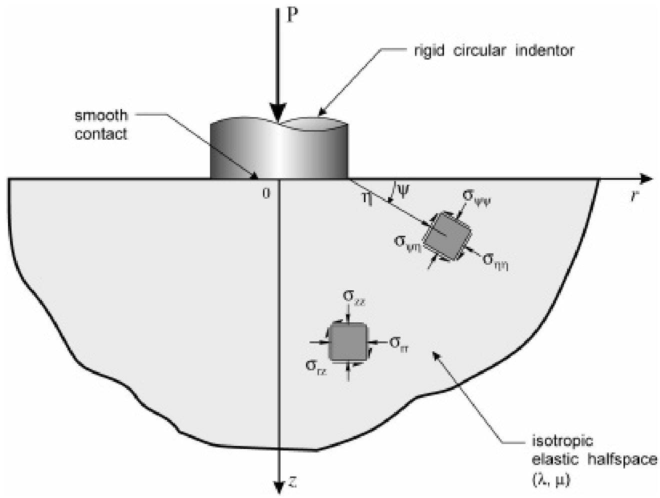

Figure 3. Local stress field at the boundary of the rigid circular indentor

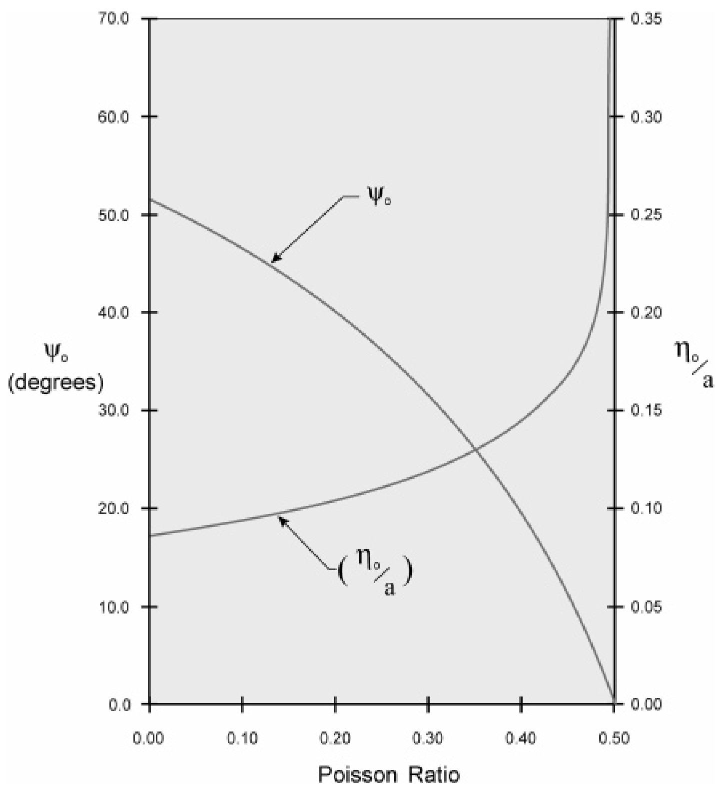

Figure 4. Location of the point of maximum tensile stress at the boundary of the rigid, smooth indentor (co-ordinates (η_0/a) and ψ are defined in Figure 3)

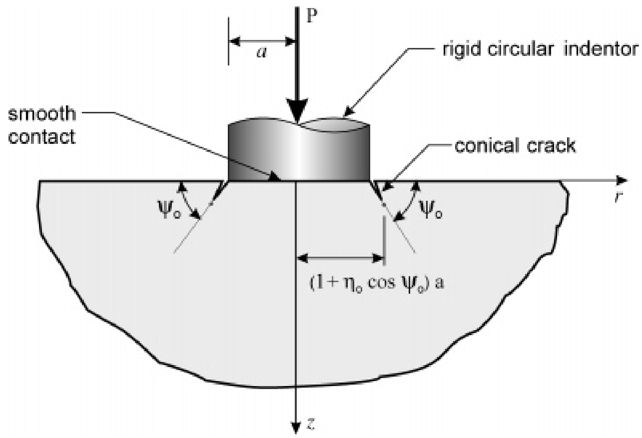

Figure 5. Starter crack configuration for the computational modelling of crack extension

(η_0, ψ_0) with an orientation normal to the direction of maximum tensile stress. The extension of such a nucleated crack will be governed by appropriate criteria governing crack extension and orientation of crack extension. In the present study we assume that, for the purposes of the study of crack extension, the nucleated crack will migrate to the edge of the contact location to form a "starter crack" (Figure 5). This methodology is certainly a proposal for the identification of the starter crack configuration required for the computational modelling of fracture extension during indentation. In situations where there is *a priori* knowledge of the orientation and length of a starter crack (e.g. results of surface seams which detect surface defects) such information could be directly used in the computational modelling procedure to specify the starter crack. The orientation of the starter crack is particularly important to the accurate modelling of the path of crack extension.

3.2. Onset of crack extension

The onset of crack extension refers to the attainment of an energy level at the crack tip which will permit the extension of the crack tip. The conditions necessary for the onset of crack extension can be specified by a variety of criteria which are based on theoretical concepts and experimental investigations conducted on brittle materials such as glass, concrete, mortar, rock and ceramics. A simple form of a criterion for the onset of crack extension can be expressed in terms of the fracture toughness of the brittle material in the crack opening mode. According to such a criterion, crack extension can be initiated when

$$K_{\mathrm{I}} = K_{\mathrm{IC}} \tag{25}$$

where K_{IC} is the critical value of the stress intensity factor in the crack opening mode. References to other criteria, including strain energy density function-based criteria, are given by Sih.[26]

3.3. Orientation of quasi-static crack growth

If we consider the development of a conoidal fracture during the indentation, in general both stress intensity factors will be present. Hence a generalized crack extension criterion should incorporate the influence of both stress intensity factors. In the current study, the orientation of quasi-static crack growth is determined by employing the criteria postulated by Erdogan and Sih.[25] The maximum stress criterion assumes that the crack will extend in the plane which is normal to the maximum circumferential stress $\sigma_{\psi\psi}$, referred to the local coordinate system (Figure 3), in accordance with the condition

$$K_{\mathrm{I}} \sin\psi + K_{\mathrm{II}}(3\cos\psi - 1) = 0 \tag{26}$$

The criterion (26) for determining the orientation of crack growth has been used quite extensively, and successfully, to determine crack extension paths in brittle elastic materials.[26,37]

As suggested by a reviewer, an alternative to the procedures utilized in this paper would be to utilize a condition of local symmetry for the determination of crack orientation. This implies that the crack will grow along a direction where, locally, K_{II} vanishes.[43] A calculation of K_{II} at certain discrete points along the crack extension paths indicates that the value of K_{II} is, within limitations of a numerical scheme, reasonably close to zero. It must, however, be pointed out that in this study the orientation path is determined from (26) as opposed to using the condition $K_{\mathrm{II}} \equiv 0$, for the calculation of orientation. The results are encouraging enough to adopt a local condition as a useful criterion for the estimation of crack path orientation.

4. NUMERICAL RESULTS

The computational methodology described in the previous sections was used to examine the problem of indentation fracture development at the boundary of the rigid circular indentor with a smooth contact surface. The fracture development during indentation will be governed by the deformability characteristics μ and ν of the brittle elastic material and the critical stress intensity factor K_{IC} which permits the extension of the crack according to criteria specified in Section 3. Figure 6 illustrates the pattern of conoidal-type axisymmetric crack extension from the boundary of the rigid circular indentor. It can be observed that the path of crack extension is considerably influenced by the Poisson's ratio of brittle elastic solid. The steepest orientation of the crack extension occurs when $\nu = 0$ and the crack extension path exhibits a noticeable curvature as $\nu \to 1/2$. As noted previously, in the limit as $\nu \to 1/2$, the theoretical formulations do not permit starter cracks to be initiated within the brittle elastic solid (i.e. $\eta_0 \to \infty$; $\psi_0 \to 0$ as $\nu \to 1/2$). Hence brittle fracture extension in an axisymmetric form is suppressed for $\nu = 1/2$. This, however, does not preclude the cases where axisymmetric starter crack configurations can exist at the surface of the half-space region due to either initial stress or shrinkage or residual stress effects. Such initial surface crack configurations are bound to be non-axisymmetric and the indentational fracture created is bound to follow a complex three-dimensional pattern. For the purposes of illustration, however, we examine the problem of the case where a ring crack is present at the boundary of the rigid smooth indentor with $\eta_0 = 0{\cdot}1$ and $\psi_0 = 90^\circ$. Figure 7 illustrates the crack extension pattern within the half-space region resulting from the indentation by a smooth rigid circular indentor. It is noted that crack extension into the half-space region has a similar pattern to that obtained through consideration of a starter crack configuration derived from developments given in Section 3.1. In this case, however, the crack extension within the half-space region is less pronounced and results in a conoidal crack configuration even for $\nu = 1/2$. The estimation of the load–displacement relationship of the indentor in the presence of a boundary fracture is of importance in connection with the application of the results to materials engineering. The stiffness of the indentor is utilized as a quality control measure in material characterization

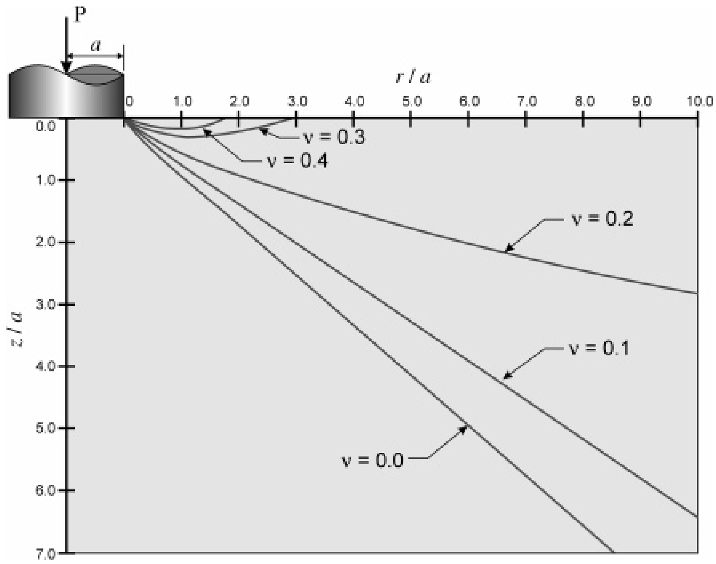

Figure 6. Pattern of conoidal crack development at the boundary of the rigid smooth indentor. (Starter crack orientation determined from Figure 4)

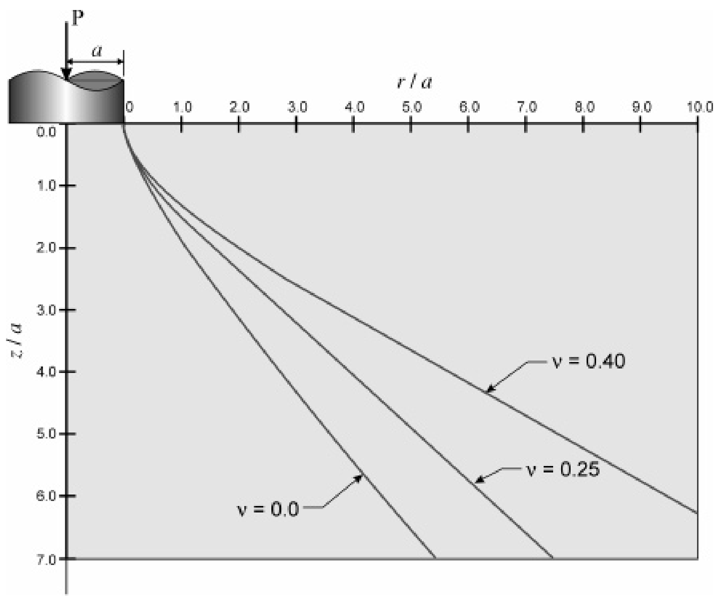

Figure 7. Pattern of conoidal crack development at the boundary of the rigid smooth indentor. (Starter crack normal to the plane boundary)

exercises. If boundary fracture effects are neglected, the interpretation of the load-displacement relationship purely by appeal to the results for an intact half-space region will be open to error. Figure 8 presents results for the load–displacement relationship for the rigid circular indentor which experiences axisymmetric boundary fracture in a conoidal shape. The load–displacement

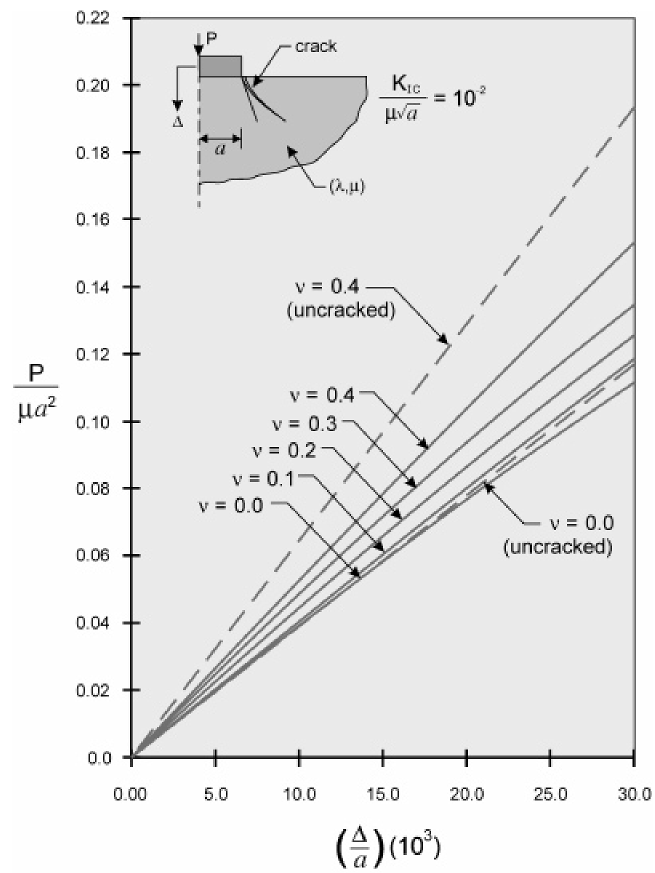

Figure 8. Influence of conoidal cracks development on the displacement behaviour of the rigid smooth indentor. [Starter crack orientation determined from considertaion of stress state (see Figure 4)]

relationship is influenced by the non-dimensional parameter $K_{IC}/\mu\sqrt{a}$, the Poisson's ratio and the orientation of the starter crack ψ_0, which itself is a function of the Poisson's ratio. The results are presented only for a specific value of the parameter $K_{IC}/\mu\sqrt{a}\,(=10^{-2})$ but are sufficient to illustrate the influence of the conoidal boundary fracture development on the indentational stiffness of the rigid circular indentor. The departure between the results for the cracked and uncracked half-space regions becomes more prominent as v increases. Figure 9 presents the results for the load–displacement relationship for the rigid circular indentor for the special case when the starter crack is oriented normal to the surface of the half-space region. In this case boundary fracture extension in a conoidal form results in a slightly greater reduction in the axial stiffness of the rigid indentor. As the magnitude of parameter $K_{IC}/\mu\sqrt{a}$ increases, axisymmetric crack development can be suppressed and the result for the load–displacement behaviour converges to that of the intact half-space region; Figure 9 illustrates such a typical result.

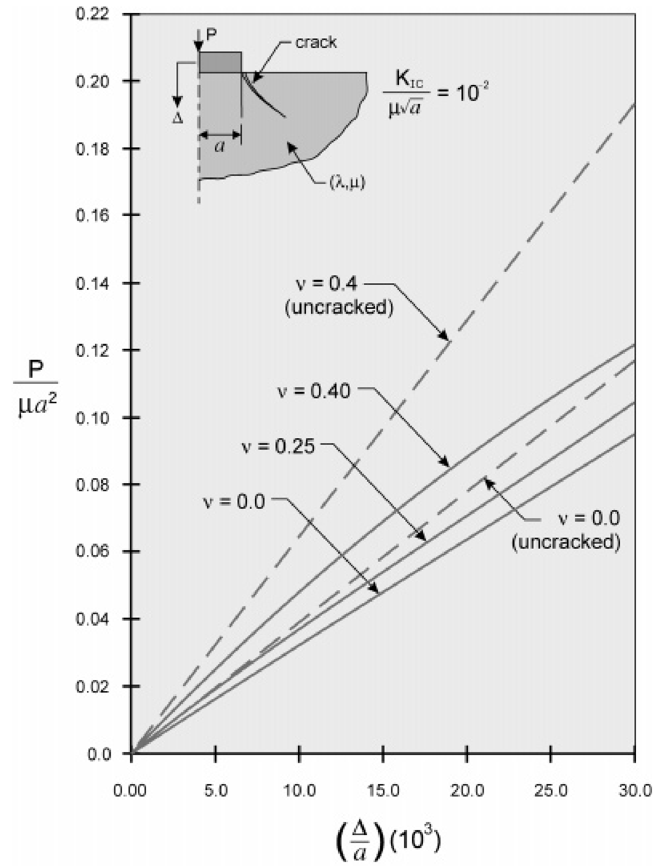

Figure 9. Influence of conoidal crack development on the rigid smooth indentor. (Starter crack normal to the plane boundary)

5. CONCLUDING REMARKS

Brittle elastic materials are susceptible to fracture during indentation by either blunt or sharp indentors. This paper focuses on the evaluation of axisymmetric quasi-static fracture evolution during indentation by a Boussinesq-type flat indentor. In general, the fracture evolution can be strongly influenced by surface defects that can be present at the surface of the half-space region. Such pre-existing surface defects will invariably result in the development of complex three-dimensional indentational fracture topography. In this paper attention is focussed on the evolution of axisymmetric indentational fracture at the boundary of a rigid flat indentor in smooth contact with a brittle elastic half-space region. When dealing with a defect free half-space region it is necessary to postulate a procedure which can be used to identify the starter crack emanating from the boundary of the indentor. The classical elasticity solution for the stress state in the vicinity of the indentor can be used to determine the location of maximum tensile stress, which in turn is used to position the starter crack for the study of fracture extension during indentation. The boundary element technique coupled with criteria for initiation of crack extension and orientation of crack extension can be conveniently adopted to examine the development of conoidal cracks at the indentor boundary. The configuration of the conoidal crack is governed by the Poisson's ratio of the brittle material and the critical stress intensity factor in the crack opening mode. These in turn influence the load–displacement response of the rigid indentor. The computational methodologies can be extended to examine the evolution of semi-circular and star-shaped three-dimensional cracks which can be initiated by pre-existing surface defects in the vicinity of the indentor.

REFERENCES

1. J. Boussinesq, *Applications des Potentiels á l'Etude de l'Equilibre et du Mouvement des Solides Elastiques*, Gautier-Villars, Paris, 1885.
2. J. W. Harding and I. N. Sneddon, 'The elastic stresses produced by the indentation of the plane of a semi-infinite elastic solid by a rigid punch', *Proc. Cambridge Philos. Soc.*, **41**, 16–26 (1945).
3. H. Hertz, 'Ueber die Berührung fester elastischer Körper', *J. Reine Angew. Math.*, **92**, 156–171 (1881).
4. A. E. H. Love, *A Treatise on the Mathematical Theory of Elasticity* , Cambridge University Press, London, 1927.
5. L. A. Galin, *Contact Problems in the Theory of Elasticity*, I. N. Sneddon, ed., North Carolina State College, Raleigh, N.C., 1961.
6. Y. S. Ufliand, *Survey of Articles on the Application of Integral Transforms in the Theory of Elasticity*, I. N. Sneddon, ed., North Carolina State College, Raleigh, N.C., 1965.
7. A. D. de Pater and J. J. Kalker eds, *The Mechanics of Contact Between Deformable Bodies*, *Proc. IUTAM Symp.*, Enschede, Delft University Press, The Netherlands, 1975.
8. A. P. S. Selvadurai, *Elastic Analysis of Soil-Foundation Interaction. Developments in Geotechnical Engineering*, Vol. 17, Elsevier Sci. Publ. Co., The Netherlands, 1979.
9. G. M. L. Gladwell, *Contact Problems in the Classical Theory of Elasticity*, Sijthoff and Noordhoff, The Netherlands, 1980.
10. K. L. Johnson, *Contact Mechanics*, Cambridge University Press, U.K., 1985.
11. J. J. Kalker, *Three-Dimensional Elastic Bodies in Rolling Contact*, Kluwer Acad. Publ. Dordrecht, The Netherlands, 1990.
12. J. C. Jaeger, *Elasticity Fracture and Flow*, Methuen, Publ. Co., London, 1962.
13. L. Elfgren, ed, *Fracture Mechanics of Concrete Structures*, *Report of the Technical Committee 90 FMA RILEM*, Chapman & Hall, London, 1989.
14. S. P. Shah, S. E. Swartz and B. Barr, eds, *Fracture of Concrete and Rock*: *Recent Developments*, *Proc. Int. Conf.*, Cardiff, Elsevier Appl. Sci., London,, 1989.
15. B. R. Lawn, *Fracture of Brittle Solids*, Cambridge University Press, U.K, 1993.
16. J. P. A. Tillett, 'Fracture of glass by spherical indentors', *Proc. Phys. Soc. Ser. B*, **69**, 47–54 (1956).
17. F. C. Roesler, 'Brittle fractures near equilibrium', *Proc. Phys. Soc. B.*, **69**, 981–992 (1956).
18. F. C. Roesler, 'Indentation hardness of glass as an energy scaling law', *Proc. Phys. Soc.*, **69**, 55–60 (1956).
19. F. C. Frank and B. R. Lawn, 'On the theory of Hertzian fracture', *Proc. Roy. Soc. Ser. A*, **299**, 291–306 (1967).
20. S. Y. Chen, T. N. Farris and S. Chandrasekar, 'Contact mechanics of Hertzian cone cracking', *Int. J. Solids Struct.*, **32**, 329–340 (1995).
21. M. M. Chaudhri and E. H. Yoffe, 'The area of contact between a small sphere and a flat surface', *Philos. Mag.*, **44**, 667–675 (1981).
22. L. M. Keer, T. N. Farris and J.-C. Lee, 'Knoop and Vickers indentation in ceramics analyzed as a three-dimensional fracture', *J. Amer. Ceramics Soc.*, **69**, 392–396 (1986).
23. B. R. Lawn and R. Wilshaw, 'Indentational fracture: principles and applications', *J. Materials Science*, **10**, 1049–1081 (1975).
24. P. Ostojic and R. McPherson, 'A review of indentation fracture theory: its development, principles and limitations', *Int. J. Fract.*, **33**, 297–312 (1987).
25. F. Erdogan and G. C. Sih, 'On the crack extension of plates under plane loading and transverse shear', *J. Basic Engng. Trans. ASME*, **85**, 519–527 (1963).
26. G. C. Sih, *Mechanics of Fracture Initiation and Propagation*, Kluwer Acad. Publ., Dordrecht, The Netherlands, 1991.
27. A. R. Ingraffea, H. N. Linsbauer and H. P. Rossmanith, 'Computer simulation of cracking in a large arch dam downstream side cracking', *Fracture of Concrete and Rock*, S. P. Shah and S. E. Swartz, eds., Springer, Berlin, pp. 334–342 (1989).
28. S. P. Shah and S. E. Swartz, eds, *Fracture of Concrete and Rock*, *SEM-RILEM Int. Conf.*, Houston, TX., Springer, Berlin, 1989.

29. A. P. S. Selvadurai and A. T. Mahyari, 'Fracture evolution during indentation of fluid saturated poroeleastic medium', *Int. J. Fract.*, **86**, 59–74 (1997).
30. T. Cruse and R. B. Wilson, *Boundary Integral Equation Methods for Elastic Fracture Mechanics*, AFOSR-TR-0355, 1977.
31. G. E. Blandford, A. R. Ingraffea and J. A. Liggett, 'Two-dimensional stress intensity factor computations using the boundary element method', *Int. J. Num. Meth. Engng.*, **17**, 387–404 (1981).
32. R. N. L. Smith and J. C. Mason, 'A boundary element method for curved crack problems in two dimensions', in *Boundary Element Methods in Engineering*, C. A. Brebbia, ed., Springer, Berlin, pp. 472–484, 1982.
33. A. P. S. Selvadurai and M. C. Au, 'Cracks with frictional surfaces: a boundary element approach', in *Proc. 9th Boundary Element Conf.*, C. A. Brebbia, ed., Springer, Berlin, pp. 211–230, 1988.
34. A. P. S. Selvadurai, 'Mechanics of a rock anchor with a penny-shaped basal crack', *Int. J. Rock Mech. Min. Sci.*, **30**, 1285–1290 (1993).
35. A. P. S. Selvadurai, 'Matrix crack extension at a frictionally constrained fiber', *J. Engng. Mat. Tech. Trans. ASME*, **116**, 398–402 (1994).
36. A. P. S. Selvadurai, 'On integral equation approaches to the mechanics of fibre-crack interaction', *Engng. Analysis with Boundary Elem.*, **17**, 287–294 (1996).
37. A. P. S. Selvadurai and A. ten Busschen, 'Mechanics of the segmentation of an embedded fiber. Part II. Computational modelling and comparison', *J. Appl. Mech. Trans. ASME*, **62**, 98–107 (1995).
38. M. H. Aliabadi, 'Boundary element formulations in fracture mechanics', *Appl. Mech. Rev.*, **50**, 83–96 (1997).
39. Th. Kermanidis, 'Numerical solution for axially symmetrical elasticity problems', *Int. J. Solids Structures*, **11**, 495–500 (1975).
40. R. D. Henshell and K. G. Shaw, 'Crack tip finite elements are unnecessary', *Int. J. Numerical Meth. Engng.*, **9**, 495–507 (1975).
41. R. S. Barsoum, 'On the use of isoparametric finite elements in linear elastic fracture mechanics', *Int. J. Numer. Meth. Engng.*, **10**, 25–37 (1976).
42. I. N. Sneddon, 'Boussinesq's problem for a flat-ended cylinder', *Proc. Cambridge. Philos. Soc.*, **42**, 29–39 (1946).
43. B. Karihaloo, 'Crack kinking and curving', *Mech. Mater.*, **1**, 189–201 (1982).
44. K. Hellan, *Introduction to Fracture Mechanics*, McGraw-Hill, New York, 1985.

